Thin Solid Films 520 (2011) 1489–1494

Contents lists available at SciVerse ScienceDirect

Thin Solid Films

journal homepage: www.elsevier.com/locate/tsf

Role of environmental and annealing conditions on the passivation-free in-Ga–Zn–O TFT

Chur-Shyang Fuh [a], Simon Min Sze [a], Po-Tsun Liu [b,*], Li-Feng Teng [c], Yi-Teh Chou [c]

[a] Department of Electronics Engineering & Institute of Electronics, National Chiao Tung University, Hsinchu 300, Taiwan, ROC
[b] Department of Photonics & Display Institute, National Chiao Tung University, Hsinchu 30010, Taiwan, ROC
[c] Department of Photonics & Institute of Electro-Optical Engineering, National Chiao Tung University, Hsinchu 30010, Taiwan, ROC

ARTICLE INFO

Available online 31 August 2011

Keywords:
Thermal annealing
InGaZnO TFT
Annealing environment
Reliability mechanism
Operation model

ABSTRACT

We examined the characteristics of passivation-free amorphous In–Ga–Zn–O thin film transistor (a-IGZO TFT) devices under different thermal annealing atmospheres. With annealing at higher temperature, the device performed better at the above-threshold operation region, which indicated the film quality was improved with the decrease of defects in the a-IGZO active region. The mobility, threshold voltage and subthreshold swing of a-IGZO TFT annealed at 450 °C was 7.53 cm^2/V s, 0.71 V and 0.18 V/decade, respectively. It was also observed that the a-IGZO was conductive after thermal annealing in the vacuum, due to the ease of oxygen out-diffusion from the a-IGZO back channel. The oxygen deficiency resultantly appeared, and provided leaky paths causing electrical unreliability when TFT was turned off. In contrast, the annealing atmosphere full of O_2 or N_2 would suppress the oxygen diffusion out of the a-IGZO back channel. The worst V_{th} degradation of a-IGZO TFT after positive gate bias stress and negative gate bias stress (NGBS) was about 2 V and −2 V, respectively. However, the V_{th} shift in the NGBS testing could be suppressed to −0.5 V in vacuum chamber. Material analysis methods including X-ray photoelectron spectroscopy and scanning electron microscopy were used to investigate the change of a-IGZO film after different thermal annealing treatments. The variation of O 1s spectra with different annealing atmospheres showed the consistence with our proposed models.
© 2011 Elsevier B.V. All rights reserved.

1. Introduction

Transparent amorphous oxide semiconductor (TAOS) has attracted a lot of attentions for its superior transparent characteristics and electrical performance, even in amorphous phase [1,2]. Among TAOS materials, amorphous indium gallium zinc oxide (a-IGZO) is one of the most popular candidates serving as semiconductor layer in thin film transistor (TFT) [1,3,4]. However, there are critical issues exhibited in the oxide TFT, especially for the absorption and desorption reaction of the oxygen atom with the surrounding atmosphere [5,6]. As the oxygen species from the ambient atmosphere are absorbed on the a-IGZO backchannel, they can capture electrons in the conducting channel and form a depletion region beneath back channel layer. By following the equation of $O_{2(g)} + e^- \leftrightarrow O^-_{2(s)}$, the resultant buildup of absorbed negative space charges $O^-_{2(s)}$ easily repells conduction electrons and positively shifts threshold voltage (V_{th}) of oxide TFT [7,8]. Previous researches on a-IGZO TFT technologies mainly focused on the electrical performance and applications, but the operation models and instability mechanism are still unclear. In this study, the operation and instability models of a-IGZO TFT can be clarifyed by adjusting experimental factors including thermal treatment processes, annealing temperatures and atmosphers. X-ray photoelectron spectroscopy (XPS) technique was used to analyze a-IGZO film before and after differenct annealing treatments. Electrical reliability test also was performed in vacuum and atmosphere chambers to study electrical reliability and the operation models of a-IGZO TFT device.

2. Experimental details

The passivation-free a-IGZO TFT with bottom gate was fabricated on a thermal oxide capped n^+ heavily doped (100) silicon substrates. First, a 100-nm-thick silicon oxide film for gate dielectric layer was thermally grown on the silicon substrate which served as the gate electrode, in a horizontal thermal furnace at 650 C. Then, a 50-nm-thick IGZO film was deposited on it by DC sputtering system with a target of the atomic ratio of In:Ga:Zn:O = 1:1:1:4. Only pure argon (Ar) gas was inserted with the deposition pressure of 3×10^{-3} Torr at room temperature. The Ar gas flow was fixed at 10 sccm. Sequentially, a 50-nm-thick ITO was formed serving as source/drain electrodes and all the layers were defined by shadow mask. The channel width and length of a-IGZO TFT were varied ranging from 1200 to 200 μm. Finally, some of the samples were thermally annealed once

* Corresponding author at: Department of Photonics and Display Institute, National Chiao Tung University, CPT Building, Room 412, 1001 Ta-Hsueh Rd. Hsin-Chu 300, Taiwan, ROC. Tel.: +886 3 5712121x52994; fax: +886 3 5735601.
E-mail address: ptliu@mail.nctu.edu.tw (P.-T. Liu).

0040-6090/$ – see front matter © 2011 Elsevier B.V. All rights reserved.
doi:10.1016/j.tsf.2011.08.088

in a vacuum furnace under a pressure of 10^{-7} Torr, and the others in the furnace with O_2 or N_2 gas flow rate of 10 L/h under the pressure of 8.7×10^{-2} Torr. Scanning electron microscopy (SEM) was used to analyze the a-IGZO films. The reliability test was conducted in a vacuum chamber which could achieve 10^{-6} Torr by the turbo molecular pumping and the atmosphere environment with a relative humidity of 50% at 25 °C. The electrical field applied to the gate electrode was given by 1 MV/cm for 180 min. All electrical measurements were carried out with a semiconductor parameter analyzer, Keithley 4200.

3. Results and discussion

Fig. 1 shows the relationship of the normalized drain current (NI_D) versus the gate voltage (V_G), at a drain-to-source voltage (V_{DS}) of 10 V for the a-IGZO TFT before and after thermal annealing at 450 °C under nitrogen, oxygen, and vacuum environments, separately. The NI_D was given by $I_D \times \frac{L}{W}$. The Improvement of the NI_D–V_G curve was clearly observed for the a-IGZO TFT with and without thermal annealing treatments. The un-annealed a-IGZO TFT had the lower driving current and the lager threshold voltage. After the thermal annealing, the on-current of a-IGZO TFT devices improved by one order of magnitude from 10^{-6} A to 10^{-5} A, and exhibited similar behavior with different annealing environments. For the O_2-annealed a-IGZO TFT and the N_2-annealed one, the NI_D–V_G curves almost were overlapped with each other, while the ones annealed in vacuum environment had larger off-current (I_{off}) than the others. These results revealed the effect of different annealing atmospheres on two electrical transport regions including the above-threshold region and turn-off region.

As the positive gate bias was applied to the a-IGZO TFT, electrons accumulated at the front channel region near the gate electrode, and formed a path for carrier transportation. The additional energy from thermal annealing process led to the material architecture rearrangement and structural relaxation, thereby reducing the defects in a-IGZO film [9–11]. This improvement of a-IGZO film quality covered the front channel region. The carrier could transfer more smoothly without being trapped in the defect centers, which led to the large turn-on current and the smaller threshold voltage. Fig. 2(a) shows the NI_D–V_G curves of a-IGZO TFT, and Fig. 2(b) and (c) sketch electrical parameters of a-IGZO TFT devices with different annealing temperatures, ranging from 250 °C to 450 °C under N_2 atmosphere. The on-current increased and threshold voltage decreased with increasing thermal annealing temperature. Besides, the subthreshold swing and on-off current ratio also improved slightly at higher annealing temperature. This indicates the predominant factor on the above-threshold characteristic was the annealing temperature, even if the

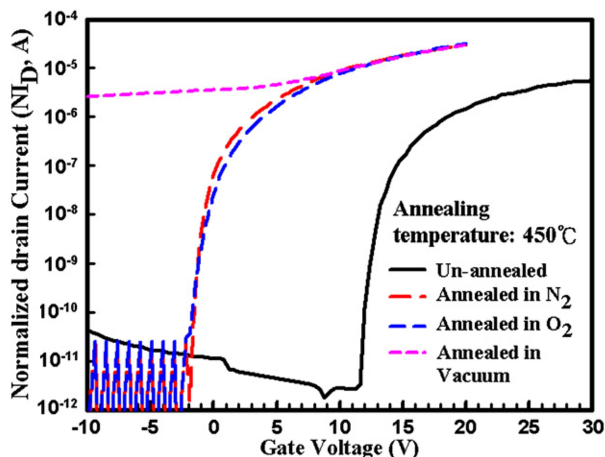

Fig. 1. Normalized I_D–V_G curves of un-annealed a-IGZO TFTs and with different annealing environments in 450 °C.

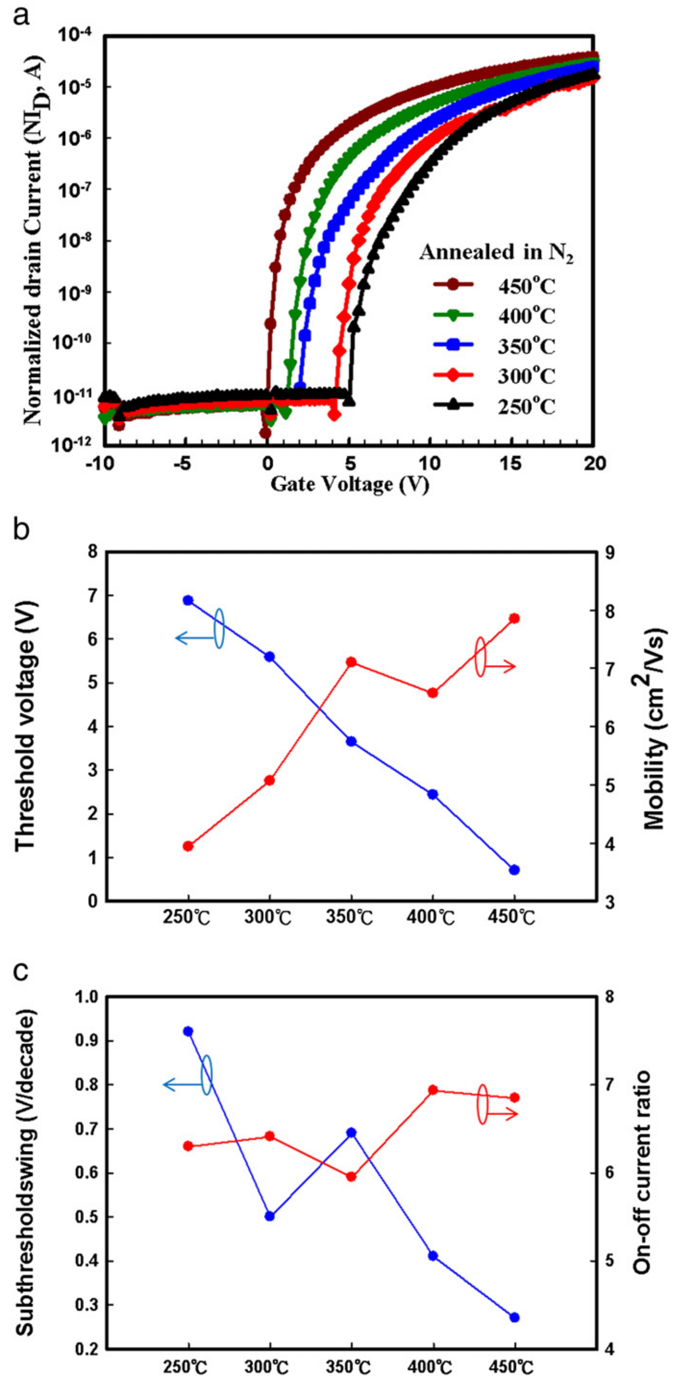

Fig. 2. (a) Immediate comparison among normalized I_D–V_G curves of a-IGZO TFTs annealed at various temperatures in N_2 atmosphere. The subpanels (b) and (c) show the threshold voltage, mobility and subthreshold swing, on-off current ratio, respectively.

annealing atmosphere was different. However, the effect of temperature couldn't completely explain the electrical performance between different annealing atmospheres. The a-IGZO TFT device annealed in vacuum couldn't be turned off easily, and behaving NI_D 10^{-6} A larger than others. In the turn-off region, the carriers in the front channel were depleted by negative gate bias and the only one path for leakage was the backchannel region. As annealing in vacuum environment, weakly bounded oxygen was easily desorbed out and formed oxygen deficiencies on the surface region of the film. Hence, the oxygen deficiencies in a-IGZO formed shallow donor states, which contributed to the enhancement of electronic conductivity [11,12]. The carriers

could easily transport at this back channel and form a larger leakage current.

The microstructure and composition of the a-IGZO films were characterized by SEM and XPS analyses. Fig. 3(a), (b), (c), and (d) shows the plane-view SEM images of a-IGZO films un-annealed, annealed at 450 °C in vacuum, O_2, and N_2, respectively. In comparison with the un-annealed sample, the morphology of IGZO with 450 °C annealing temperatures were dense and uniform, which indicated that the improvement of above-threshold characteristics could not be attributed to the formation of polycrystalline IGZO in their channels. Fig. 4 shows the results of the XPS analysis on O 1s spectrum in a-IGZO film. The O 1s peaks of a-IGZO with different annealing treatments were shown in Fig. 4(a). This indicated the thermal annealing treatment truly altered the oxygen bonding and composition in the a-IGZO and changed their characteristics. For a detailed analysis, the spectra of the a-IGZO films un-annealed, annealed in vacuum, O_2, N_2 were shown in Fig. 4(b), (c), (d) and (e), respectively. Three distinct components of O 1s peak at the surface could be fitted by Gaussian Lorentzian deconvolution, which centered at 530.6 ± 0.3 (peak A), 531.5 ± 0.2 (peak B) and 532.6 ± 0.3 (peak C) eV, respectively. The low binding energy of O 1s spectrum at 530.6 ± 0.3 eV is attributed to O^{2-} ions on wurtzite structure of hexagonal Zn^{2+} ion array surrounded by Zn atoms [13]. This indicated the oxygen formed a bonding with Zn atom in the a-IGZO film. The medium binding energy of the spectrum at 531.15 ± 0.2 eV may be associated with O^{2-} ions in the oxygen deficient regions within the matrix of the a-IGZO film [14,15]. The highest binding energy peak at 532.6 ± 0.3 eV is usually attributed to the presence of loosely bound oxygen on the surface or micro pores of the a-IGZO film, belonging to hydrated oxides species such as adsorbed CO_3, H_2O, and O_2 [13].

As seen in Fig. 4(b) and (c), the intensity ratio of peak A to peak B apparently decreased after the thermal annealing in vacuum, which indicated the amount of oxygen deficiencies increased. With thermal energy, the oxygen atoms are easily desorbed out of the surface of a-IGZO without any obstructions, which is consistent with the observed variation in the electrical performance. The backchannel of a-IGZO layer was formed a leaky path when the TFT operated at turn-off region. In Fig. 4(d) and (e), the curve fitting also revealed the amount of oxygen deficiencies decreased after annealing in O_2 and N_2 environments. The intensity ratio of peak A to peak B increased apparently, which indicated the oxygen deficiencies was fewer than the film annealed in vacuum. When annealed in O_2 and N_2, the gas pressure in the chamber can depress the oxygen desorption from the a-IGZO surface. Besides, the oxygen and nitrogen molecular in the chamber could fill in the sites of oxygen vacancies generated at high temperatures [16]. Hence, with less oxygen deficient, the back channel of a-IGZO TFT could be turned off with small leakage current as compared with the thermal annealed one in vacuum.

To confirm the results in above experiment, an environment-dependent reliability test was performed to the a-IGZO TFT. As in the previous researches on oxide semiconductors, the oxygen species from the ambient atmosphere absorbed into the oxygen deficiencies at the back channel can capture electrons in the oxide semiconductor, and generate the negatively charged species ($O^-_{2(s)}$), as described by the following chemical reaction:

$$O_{2(g)} + e^- \leftrightarrow O^-_{2(s)}, \quad (1)$$

where e^- denotes electrons. $O_{2(g)}$ and $O^-_{2(s)}$ represent the neutral and charged oxygen molecules in the film of a-IGZO TFT. Under positive gate bias stress (PGBS), more electrons induced in the bulk and formed the negatively charged species ($O^-_{2(s)}$), which easily repelled conduction electrons in the front channel and cause the positive V_{th} shift in TFT [7,8]. Fig. 5 shows the V_{th} shift after gate bias stress with different annealing treatments, and be tested in different environments. Fig. 5(a) and (b) presented the electrical reliability in atmosphere and vacuum chamber,

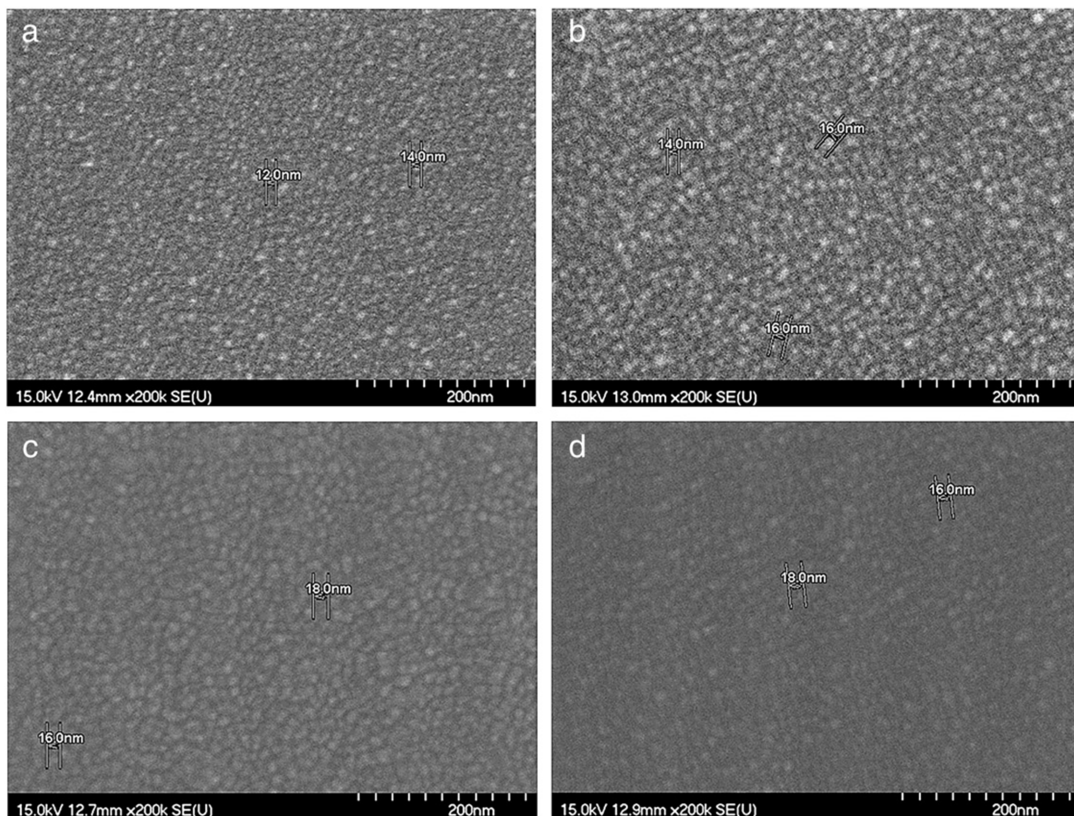

Fig. 3. SEM images of surface morphology of (a) un-annealed a-IGZO films and films annealed in (b) vacuum, (c) O_2, and (d) N_2.

Fig. 4. XPS O 1s spectrum of a-IGZO films (a) with different annealing environments, the detail curve fitting of results of (b) un-annealed, (c) vacuum annealed, (d) O_2 annealed and (e) N_2 annealed a-IGZO films.

respectively. The value of V_{th} shift was about 2 V for the O_2 and N_2 annealed devices under PGBS. It indicated a fewer oxygen absorbed and transfer to negatively charged species ($O^-_{2(s)}$) in a-IGZO film. By comparing Fig. 5(a) and (b), the shift values of V_{th} were almost the same, which implied the amount of negatively charged species ($O^-_{2(s)}$) formed in the films was similar. The a-IGZO TFTs annealed in O_2 and N_2 performed better quality with less oxygen deficiencies at the back channel than the one annealed in vacuum. The V_{th} shift under the NGBS tests in atmosphere and air was apparently larger than in vacuum. If the amount of absorbed species was confined in the reliability tests, the negative gate bias could depleted the electron and prevented the formation of negatively charged species ($O^-_{2(s)}$) where the V_{th} should not positively shift.

Under the NGBS, another mechanism could dominate over the a-IGZO film. Moisture ($H_2O_{(g)}$) adsorption from the atmosphere could form positively charged species ($H_2O^+_{(s)}$) in the surface of film. The reaction process is proposed as follows:

$$H_2O_{(g)} \leftrightarrow H_2O^+_{(s)} + e^-, \qquad (2)$$

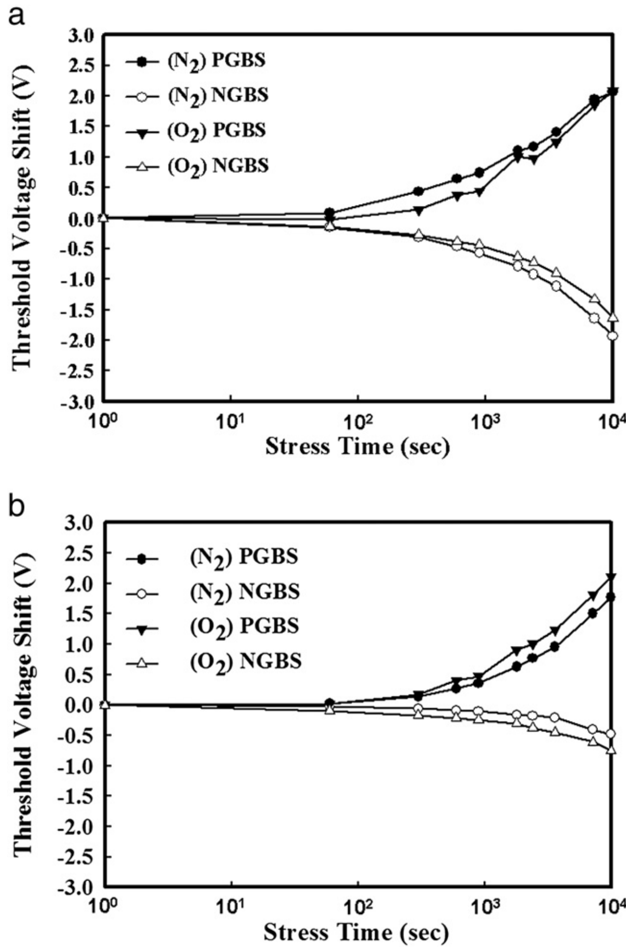

Fig. 5. Variation in V_{th} of a-IGZO TFTs with time, to which gate bias stress was applied in (a) ambient and (b) vacuum chambers in dark environment.

where $H_2O_{(g)}$ and $H_2O^+_{(s)}$ represent the neutral and positively charged water molecules, respectively. The $H_2O_{(g)}$ absorbed at the back surface of channel layer forms $H_2O^+_{(s)}$ as electron donors and the carriers in the film, which could easily accumulate the electron channel in a-IGZO film [6,17]. This phenomenon causes the negative shift of V_{th} under the NGBS. Besides, the absorbed water molecules were charged at the back surface of the film. It explains that the V_{th} shift was independent of the annealing atmosphere either in O_2 or N_2, even if the oxygen vacancies in a-IGZO film decreased. This could also explain the smaller V_{th} shift of the device stressed in vacuum. The moisture was pumped out of the chamber and limited the amount of moisture absorbed at the back surface of a-IGZO film. The value of V_{th} shift was −0.5 V in this environment and smaller than the one stressed in atmosphere.

To coordinate the results in above experiment, we propose an operation model to describe the electric performance in the passivation-free a-IGZO TFT. Fig. 6 shows the schematic cross section of the IGZO TFT. The black ellipse and triangle represent the absorbed gas species and moisture in the schematic, respectively. According to the electrical measurement, the channel could be divided into two parts, front channel and back channel. The region in the bottom of the a-IGZO film, the front channel, was controlled by the gate electrode. Its quality affects the characteristic of the above threshold region, such as on current and mobility, and could be improved by thermal annealing. In the upper side of the a-IGZO film, the back channel, the gate induce electric field could not totally control the carrier and might cause a leakage path by forming excess oxygen deficiencies in thermal annealing. Besides, it also affects the PBGS reliability of the a-IGZO TFT by absorbing oxygen species in ambient. However, the back surface of the film influenced the NBGS reliability by absorbing moisture in the ambient. The degradation could not be released easily only by adjusting thermal annealing temperatures and atmospheres if separating the moisture from the back surface of a-IGZO layer.

4. Conclusion

The passivation-free a-IGZO TFT after different annealing conditions was studied by SEM, XPS analysis and electrical reliability measurements. The NI_D–V_G curve shows an apparently higher leakage current after the annealing in vacuum than the annealed one in O_2 or N_2. In XPS O 1s spectra, it was found that the intensity of the sub-peak at 531.5 eV of the a-IGZO film annealed in vacuum was apparently larger than the others. It also indicated the large amount of oxygen desorption out of the a-IGZO film occurred during the vacuum annealing, and generating oxygen deficiencies left in the backchannel. The relationship between electrical characteristics and thermal annealing temperatures can be well explained in the above-threshold operation region. With annealing at high temperature in the O_2 or N_2 atmospheres, the defects were reduced by structural relaxation and perform stronger bonding between the oxygen atoms and Zn atoms in a-IGZO film. Material analysis thereby exhibit the sub-peak intensity at 530.5 eV was larger than the film annealed in vacuum. The reliability test suggested that the oxygen deficiencies were filled with oxygen or nitrogen atoms, and thereby the difference of V_{th} shift after gate bias stress was hardly observed between the TFTs annealed in O_2 and N_2. Finally, the operation and instability models were reasonably proposed for the passivation-free a-IGZO TFT in the present work.

Acknowledgment

The authors would like to thank the National Science Council of the Republic of China, Taiwan for financially supporting this research

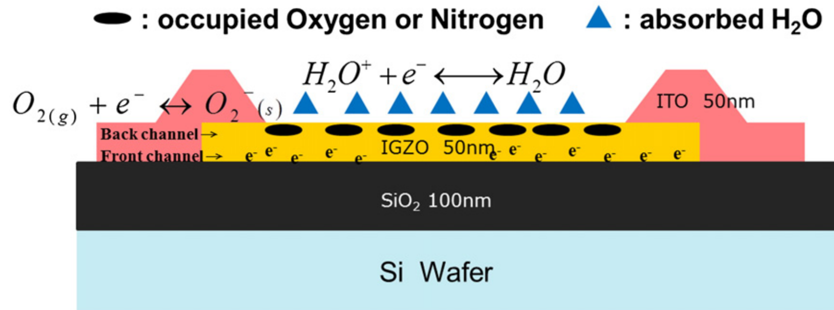

Fig. 6. Schematic operation model of a-IGZO TFTs. The inset formulae show the environment-dependent surface reactions.

under Contract No. NSC 100-2628-E-009-016-MY3. Also, this work was performed at National Nano Device Laboratories, Taiwan, ROC.

Reference

[1] K.B. Park, J.B. Seon, G.H. Kim, M. Yang, B. Koo, H.J. Kim, M.K. Ryu, S.Y. Lee, Electron Device Lett. 31 (4) (April 2010) 311.
[2] T. Kamiya, H. Hosono, NPG Asia Mater. 2 (1) (2010) 15.
[3] J.S. Lee, S. Chang, S.M. Koo, S.Y. Lee, Electron Device Lett. 31 (3) (March 2010) 225.
[4] C.J. Chiu, S.P. Chang, S.J. Chang, Electron Device Lett. 31 (11) (November 2010) 1245.
[5] D. Kang, H. Lim, C. Kim, I. Song, J. Park, Y. Park, Appl. Phys. Lett. 90 (192101) (2007).
[6] Y.C. Chen, T.C. Chang, H.W. Li, S.C. Chen, J. Lu, W.F. Chung, Y.H. Tai, T.Y. Tseng, Appl. Phys. Lett. 96 (2010) 262104.
[7] P.T. Liu, Y.T. Chou, L.F. Teng, C.S. Fuh, Appl. Phys. Lett. 94 (2009) 242101.
[8] P.T. Liu, Y.T. Chou, L.F. Teng, Appl. Phys. Lett. 95 (2010) 233505.
[9] T. Kamiya, K. Nomura, H. Hosono, J. Disp. Technol. 5 (12) (2009).
[10] P.T. Liu, Y.T. Chou, L.F. Teng, C.S. Fuh, Appl. Phys. Lett. 97 (2010) 083503.
[11] P. Barquinha, L. Pereira, G. Gonçalves, R. Martins, E. Fortunato, Electrochem. Solid-State Lett. 11 (2008) H248.
[12] H. Omura, H. Kumomi, K. Nomura, T. Kamiya, M. Hirano, H. Hosono, J. Appl. Phys. 105 (2009) 093712.
[13] K.H. Kim, G.H. Kim, H.J. Kim, Phys. Status Solidi (7) (2010) 1660.
[14] M.C. Chen, T.C. Chang, S.Y. Huang, S.C. Chen, C.W. Hu, C.T. Tsai, S.M. Sze, Electrochem. Solid-State Lett. 13 (2010) H191.
[15] K. Nomura, T. Kamiya, E. Ikenaga, H. Yanagi, K. Kobayashi, H. Hosono, J. Appl. Phys. 109 (2011) 073726.
[16] Liu Po-Tsun, Chou Yi-Teh, Teng Li-Feng, Li Fu-Hai, Shieh Han-Ping, Appl. Phys. Lett. 98 (2011) 052102.
[17] M.E. Lopes, H.L. Gomes, M.C.R. Medeiros, P. Barquinha, L. Pereira, E. Fortunato, R. Martins, I. Ferreira, Appl. Phys. Lett. 95 (2009) 063502.